DE GRUYTER Chemistry Teacher International 2021; 3(2): 117–129

Special issue paper

Suhaila Idayu Abdul Halim, Chin Han Chan* and Jan Apotheker

Basics of teaching electrochemical impedance spectroscopy of electrolytes for ion-rechargeable batteries – part 2: dielectric response of (non-) polymer electrolytes

https://doi.org/10.1515/cti-2020-0018
Received August 8, 2020; accepted April 26, 2021; published online May 27, 2021

Abstract: In the Part 2 of this article, we present the phenomenological response of the dielectric relaxation for polymer electrolytes monitored by electrochemical impedance spectroscopy (EIS) in terms of electrochemical point of view, such as impedance (Z^*), permittivity (ε^*), loss tangent ($\tan \delta$), modulus (M^*) and conductivity (σ^*) spectra. It is noteworthy to note that all the electrochemical aspects mentioned are of interest for conduction and seen as closely related to each other indirectly or directly. Two different systems; solid polymer electrolyte (SPE) [poly(ethylene oxide) (PEO) + lithium perchlorate ($LiClO_4$)] and non-SPE [poly(methyl acrylate) (PMA) + $LiClO_4$] were employed for discussion. EIS is a powerful technique to characterize the electrical properties of polymer electrolytes. The results suggest that impedance and modulus are of interest for decoupling of dielectric and electric properties by evaluating the short-range and long-range mobility of the charged entities, respectively. One is able to identify the conduction mechanism of the polymer electrolytes easily if the responses are well understood. The objective of this article to introduce a simplified yet an insightful background and technique that is easy to be followed and useful for educational purposes especially for beginners or young researchers for both undergraduates and postgraduates.

Keywords: Debye response; dielectric relaxations; electrochemical impedance spectroscopy; polymer electrolytes.

Introduction

The basics of electrolytes, electrochemical impedance spectroscopy (EIS) instrumentation and some fundamental background on electrolytes and batteries were elucidated in the Part 1 of this article. This

---

This is one of the instructor's notes based on the short course presented at the 25th POLYCHAR 2017 World Forum on Advanced Materials, Kuala Lumpur, Malaysia, October 9–13, 2017. The power point slides can be accessed *via* https://iupac.org/wp-content/uploads/2017/12/IUPAC_PolymEdu_Shortcourse_1ppt_ChinHanChan.pdf and the QR code:

***Corresponding author: Chin Han Chan**, Faculty of Applied Sciences, Universiti Teknologi MARA, 40450 Shah Alam, Selangor, Malaysia, E-mail: cchan_25@yahoo.com.sg. https://orcid.org/0000-0003-0990-0155
Suhaila Idayu Abdul Halim, Faculty of Applied Sciences, Universiti Teknologi MARA, 40450 Shah Alam, Selangor, Malaysia
Jan Apotheker, Faculty of Sciences and Engineering, University of Groningen, 9747 AG, Groningen, Netherlands

article comprises two parts; Part 1 elucidates on good practical approach to estimate the electrical bulk properties of polymer electrolytes *i.e.* bulk resistance (R_b), that is inversely proportional to the conductivity (σ_{DC}) using different approaches and Part 2 illuminates more on the phenomenological changes of the charged entities of polymer electrolytes *i.e.* dielectric and electric relaxations, under an effect of oscillating electric field. This phenomenological point of view is addressed and highlighted systematically in the classic sense, in terms of impedance (Z^*), permittivity (ε^*), loss tangent ($\tan\delta$), modulus (M^*) and conductivity (σ^*) spectra.

Solid polymer electrolytes (SPEs) are usually formed by dissolution of inorganic salts in the polymers (Agrawal & Pandey, 2008; Alloin, D'Aprea, Kissi, Dufresne, & Bossard, 2010; Armand, 1986; Berthier et al., 1983; Chin Han Chan & Kammer, 2008). SPEs are seen as the potential candidate for the modern lithium ion (Li-ion) battery because in some cases they are able to perform as ionic conductors (Li, Chen, Fan, Kong, & Lu, 2016; Scrosati, Croce, & Panero, 2001). Since 40 years ago, poly(ethylene oxide) (PEO) has gained much popularity as a good polymer host for highly efficient SPEs for solid state devices *e.g.* lithium ion (Li-ion) rechargeable batteries, due to its higher solvation effect with a lot of inorganic salt (*e.g.* lithium salt, sodium salt *etc.*) (Abraham & Jiang, 1996; Chan et al., 2014; Das, Thakur, & Kumar, 2013; Harun, Chan, & Winie, 2017; Hassoun & Scrosati, 2010). The binary polymer-salt systems under the discussion of this article are the high molar mass semi-crystalline polymer, *i.e.* PEO (possess of crystalline and amorphous regions) and the amorphous polymer, *i.e.* poly(methyl acrylate) (PMA) of which both polymers were added with lithium salt (Li-salt), *i.e.* lithium perchlorate ($LiClO_4$). It is widely known that ionic conduction takes place in the amorphous region (Chan, Sulaiman, Kammer, Sim, & Harun, 2011; Halim, Chan, & Winie, 2017; Karim, Sim, Chan, & Ramli, 2015; Pratap & Chandra, 2013). In this case, the percolation pathway takes place in the amorphous region of semi-crystalline PEO and PMA. PEO-$LiClO_4$ system at room temperature is seen as heterogenous not only with respect to morphology (semi-crystalline), but also from electrical point of view. Double-layer capacitance resulting from polarization of charges can be seen not only at the electrolyte-electrode interfaces but also at the grain boundaries of amorphous and crystalline regions (Chan & Kammer, 2018; Wang et al., 2014). The conduction mechanism of PEO-$LiClO_4$ at room temperature may be ruled chiefly by dielectric relaxation (polarization of the charged entities in the short-range motion), and the electric relaxation (flow of charged entities in the long-range motion) may start to become significantly important only when the system is in the molten state (above the melting point of PEO) (Chan & Kammer, 2016; Kammer, 2017). The second binary polymer-salt system under discussion is PMA-$LiClO_4$. PMA is an amorphous polymer (Mead & Fuoss, 1942). Addition of Li-salt in PMA leads to small-scale interaction between PMA and Li-salt (Abdul Halim, Chan, & Kammer, 2019; Halim et al., 2017). The salt molecules in PMA are seen as slightly inactive as compared to PEO (Abdul Halim et al., 2019). The system may exhibit both resistive and capacitive behavior with comparative dielectric constant as PEO (at low content of salt) only after addition of high content of Li-salt. However, the binary PMA-$LiClO_4$ system does not form any double-layer capacitance at the electrode-electrolyte interface even at high salt content under the experimental condition of this study.

Most of the solid polymer electrolytes, we merely have randomly oriented charged entities (dipoles) that generally interacting with each other, and these charged entities are seen to be aligning towards the direction of the oppositely charged electrodes under action of external electric field (Billah, 2019; Chan & Kammer, 2018; Kammer, 2017). However, in most cases, these dipolar entities are immobilized and gain mobility only due to the polymer chain relaxation (Martwiset et al., 2009; Pulst et al., 2016). For PEO, it seems with tiny fraction of salt molecules dissolved in, it becomes electrically active in promoting conductance (Berthier et al., 1983; Christie, Lilley, Staunton, Andreev, & Bruce, 2005; Pratap & Chandra, 2013). Most of the times, electrode polarization (or double-layer capacitance effect) in polymer electrolyte may provide some insight on the conduction mechanism of the systems.

EIS has been adopted to elucidate the dielectric and electrical relaxations in SPE and non-SPE. EIS data may be presented as Nyquist plot (refer to the Part 1 of this article) or Bode plot (Bode, 1945). For Nyquist plot, frequency is hidden whereas for Bode plot, frequency is explicit. These two plots are essentially of the interest in elucidation of electrical and dielectric properties of the electrolytes and their interfaces with the electrodes

(Chin Han Chan & Kammer, 2015, 2018, 2020). The Nyquist plot illuminates on the electrical bulk properties of the electrolytes, *i.e.* bulk resistance (R_b). The Bode plot, illuminates more on the time response or dielectric relaxation time of the electrolytes. The basic concept, mechanism and characteristic of dielectric materials, dielectric relaxation and polarization aided with schematic illustrations were shown and explained in a simpler manner in the Part 1 of this article (Abdul Halim, Chan, & Apotheker, 2020). For polymer electrolytes, there are several distinctive resonances that can be scrutinized under an action of externally imposed frequency (the oscillating electric field). These resonances frequently imply to dipoles relaxation at particular frequency, which allows the decoupling of small-scale electrode polarization at the electrode–electrolyte interface and conductance within the electrolyte (*i.e.* the dielectric relaxation, electric relaxation, and electrode polarization). Hence, we note here, the frequency-dependent impedance and modulus spectra are the key quantities of interest to decouple the short-range (local motion) and long-range (non-local motion) dielectric properties of electrolytes and their interfaces with the electrodes. There are few other methods that can be utilized to understand the dynamics of dipolar entities and polymer chain segmental motions such as solid-state nuclear magnetic resonance (NMR), neutron scattering, and small-angle X-ray scattering (SAXS) *etc.* (Chen et al., 2019, 2021; Wang, Xia, Chen, & Yoa, 2020). We address this situation by not focusing on ions, dipoles, super molecular structures *etc.* Instead, we made impedance measurements, where an electric field was applied to the dielectric materials. We elucidate the dielectric behavior as fluctuation and dissipation behavior in thermodynamics sense.

The understanding on conduction mechanism of polymer electrolytes from a molecular point of view has yet to be well understood and requires further exploration. It is mainly due to the nature of charge entities is not well understood. We may have molecular interaction of polymer chains with salt molecules leading to the presence of dipolar entities (Chin Han Chan & Kammer, 2018; Kammer, 2017). It is rather challenging to describe this complex situation from a molecular point of view even for binary polymer-salt systems. Therefore, we present a phenomenological point of view resulting from development of polarization, alignment, and relaxation of the charged entities (dipoles or dipolar entities). The following discussion has been kept in terms of electrochemical and electrical in order to familiarize beginners and young researchers, alongside to serve as an alternative reference for course instructors to coach their students on the subject matter.

Basics – electrochemical terms

In principle, the conductance mechanism of polymer electrolytes originates from reorientation of charged entities (dipoles or dipolar entities) when placed under an action of oscillating electric field. For impedance spectroscopy, the polymer electrolyte forms a parallel plate capacitor with the two blocking electrodes with area (A) and thickness (ϑ). Hence, the complex capacitance (C^*) can be seen as

$$C^* = \varepsilon^* C_o = \varepsilon^* \varepsilon_o \frac{A}{\vartheta} \tag{1}$$

with $C_o = \varepsilon_o (A/\vartheta)$ read as the geometric capacitance in vacuum and $\varepsilon_o = 8.854 \cdot 10^{-12}$ F m^{-1} as permittivity in vacuum. Equation (1) elucidates that the complex permittivity (ε^*) is seen to be closely related to complex impedance (Z^*), where both parameters are seen as the central quantities of impedance spectroscopy, as reflected from Equation (1). Under dynamic course, the interrelation between impedance and permittivity is given by

$$Z^* = \frac{1}{\dot{C}^*} = \frac{1}{i\omega C_o \varepsilon^*} \tag{1a}$$

with $\dot{C}^*$ being derivative of capacitance with respect to time. Therefore, under the effect of sinusoidal electric field, EIS data of the measured quantity might be portrayed and discussed according to the subsequent symmetric formulations

$$\begin{aligned}
&\text{Impedance} \quad Z^* = Z' + iZ'' = \frac{1}{i\omega C_0 \varepsilon^*} \\
&\text{Permittivity} \quad \varepsilon^* = \varepsilon' - i\varepsilon'' = \frac{1}{i\omega C_0 Z^*} \\
&\text{Electric modulus} \quad M^* = M' + iM'' = \frac{1}{\varepsilon^*} = i\omega C_0 Z^* \\
&M' = C_0 \omega Z'' \quad M'' = C_0 \omega Z' \\
&\tan\delta = \frac{\varepsilon''}{\varepsilon'} = \frac{M''}{M'} = \frac{Z'}{Z''}
\end{aligned} \tag{2}$$

where, X' and X'' denote real and imaginary parts of quantity X, ω and f denote as angular frequency and frequency, respectively, with $\omega = 2\pi f$. All quantities of Equation (2) are closely interrelated to each other as well as to complex conductivity, where

$$\begin{aligned}
&\sigma^* = i\omega\varepsilon_0\varepsilon^* \quad M^* = i\omega C_0 Z^* \\
&\sigma' = \frac{\vartheta}{A}\frac{Z'}{|Z|^2} \quad \sigma'' = \frac{\vartheta}{A}\frac{Z''}{|Z|^2} \\
&\sigma_{\mathrm{DC}} \propto \varepsilon''\omega
\end{aligned} \tag{3}$$

From the above formulations, we see that Z^* and $\varepsilon^*$are the central quantities of EIS measurement, which is presented in Equation (1). Equation (1) tells that capacitance $C' \propto \varepsilon'$ and $C'' \propto \varepsilon''$, where ε' and ε'' are denote as the stored and the dissipated energy for conductance, respectively. As a whole, the quantities can be interpreted as follows:

- Z' can be seen as Ohmic resistance
- Z'' can be seen as non-Ohmic resistance. This quantity can be seen as the capacity resistance resulting from the polymer electrolyte acts as capacitor in EIS. It displays several characteristic frequencies *e.g.* “dielectric” relaxation as the consequence of *local motion* (short-range mobility) of the charged entities
- ε' is known as the dielectric constant at $\varepsilon'(f \rightarrow \infty)$ with f note as frequency. This quantity indicates the ability of the polymer to store energy reversibly under the action of oscillating electric field
- ε'' denotes as the dielectric loss (or dissipation of energy). The finite displacement of charged entities (or dielectric polarization) of a polymer electrolyte may differ under the induced oscillating electric field as an effect of the energy dissipation, that occurs due to flowing of charged entities, ionic conduction, or conversion into thermal energy (*via* molecular vibration)
- M'' is seen as directly proportionate to Z'. Hence, M'' illuminates the “electric” relaxation of the flowing charged entities resulting from *non-local motion* (long-range mobility). The resonance appears when the externally induced sinusoidal AC frequency matches with the dielectric relaxation frequency
- σ' is coined by flow of charges (dissipation of charges)
- σ'' reflects storage of charges

The EIS is recognized as a powerful tool for evaluation of electric and dielectric properties of the measured quantity and their interfaces with conducting electrodes. For polymer electrolytes, the electric and dielectric properties are evaluated from the consequence of alignment of the charged entities (dipoles) after externally imposed to alternating frequency. Therefore, the emphasis of the following discussion is on the response of the charged entities in the solid polymer electrolytes (*i.e.* SPE: PEO-$LiClO_4$ and non-SPE: PMA-$LiClO_4$) under the effect of oscillating electric field in classical sense (*i.e.* to decouple the short-range and long-range dielectric relaxation resulting from local or non-local motion of the charged entities).

Experimental

The preparation of SPE and non-SPE used for this publication were published elsewhere (*i.e.* dissolution of $LiClO_4$ in PEO and PMA, respectively) (Halim et al., 2017). The experimental procedures using electrochemical impedance spectroscopy can be found in the Part 1 of this article. Data were extracted from Part 1 of this article. Hence, we exclude the experimental details in the Part 2 of this article. Here, we list only the polymer hosts, frequency range and temperature for EIS measurement (*c.f.* Table 1). In the following section, we discuss the impedance data of the systems given in Table 1.

Table 1: Characteristics of polymer electrolytes.

Polymer	Molar mass (g mol^{-1})	W_S[a]	Frequency range (Hz)	T[b] (°C)	T_g[c] (°C)	T_m[d] (°C)
PEO	300,000	0.5 wt.% and 11 wt.%	50–2 MHz	25	−56	65
PMA	40,000	2 wt.% and 11 wt.%	50–2 MHz	25	13	–

[a] Salt content estimated from percentage of mass of salt/(mass of polymer + salt); salt: $LiClO_4$. [b] Temperature for EIS measurement. [c] Glass transition temperature estimated using differential scanning calorimetry (Abdul Halim et al., 2019). [d] Melting temperature estimated using differential scanning calorimetry (Halim et al., 2017).

Results and discussion

We note here the binary polymer-salt systems (*i.e.* PEO-$LiClO_4$ and PMA-$LiClO_4$) with 0.5 wt.% of $LiClO_4$ as low salt system and 11 wt.% of $LiClO_4$ as high salt system. These notations are applied throughout the discussion.

Impedance

The frequency-dependent impedance spectra of polymer electrolytes monitored by EIS *i.e.* Bode plots of PEO-$LiClO_4$ (SPE) and PMA-$LiClO_4$ (non-SPE), are displayed in Figure 1. Normally, in a Bode plot, one may observe several characteristic frequencies at a particular frequency resulting from electrode polarization or dielectric relaxation of charged entities (we named here dipolar entities).

We note the double-logarithmic plot of impedance spectra presented in Figure 1(a) as:

- Both PEO-$LiClO_4$ systems (*i.e.* in addition of 0.5 wt.% and 11 wt.% of $LiClO_4$) have an average maximum resonance in Z'' spectrum at certain frequency region noted as $f_{\mathrm{max}}^{Z''}$, this is as a result from the relaxation of dipolar entities. Hence, we may describe the orientation of dipolar entities in PEO-$LiClO_4$ is dominantly restricted to short-range motion (local motion) and insignificant long-range motion as the dipoles fully oriented/relaxed at high frequency region.
- The systems possess one intersection point of Z' and Z'' spectrum at a frequency region noted as $f_{\mathrm{cross}}^{Z'-Z''}$. The distance of $f_{\mathrm{max}}^{Z''}$ and $f_{\mathrm{cross}}^{Z'-Z''}$ is seen to broaden with elevating salt content.
- Both systems have an average minimum resonance in Z'' spectrum at a lower frequency region noted as $f_{\mathrm{min}}^{Z''}$. The minimum at $f_{\mathrm{min}}^{Z''}$ normally reflects to the accumulation of dipoles at the electrode-electrolyte interface (electrode polarization or double-layer capacitance). This phenomenon will normally result in distribution of (dielectric) relaxation times in the SPE. The experimental fact of electrode polarization, frequently seen as a nuisance in use of polymer electrolytes, but it actually plays an important role in our understanding of conductivity.
- The three characteristic frequencies *i.e.* $f_{\mathrm{min}}^{Z''}$, $f_{\mathrm{max}}^{Z''}$ and $f_{\mathrm{cross}}^{Z'-Z''}$ [*c.f.* Figure 1(a) and (b)] increase to higher frequency range, alongside with distancing of $f_{\mathrm{max}}^{Z''}$ and $f_{\mathrm{cross}}^{Z'-Z''}$ [*c.f.* Figure 1(b)] with increasing of salt content.
- The systems are noted with large distribution of relaxation times with increasing salt content $f_{\mathrm{max}}^{Z''} < f_{\mathrm{cross}}^{Z'-Z''}$. This phenomenon is seen as deviation from Debye response because the system possesses more than one

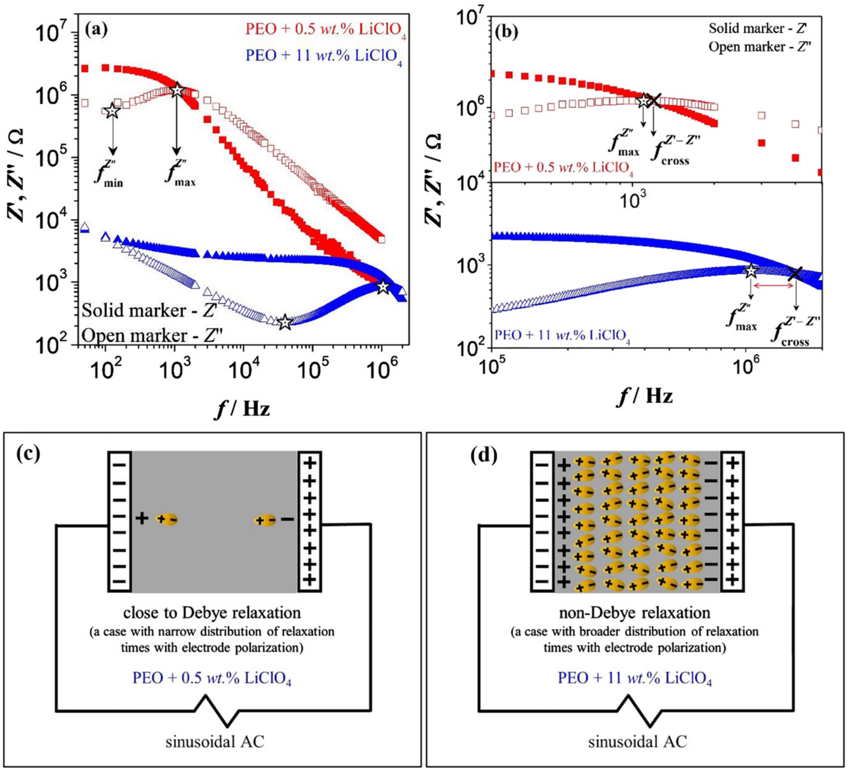

Figure 1: Frequency-dependent impedance spectra of (a) PEO-LiClO$_4$, (b) zoom-in of PEO-LiClO$_4$, and schematic illustration of dipolar entities orientation of the respective systems, where (c) close to Debye response and (d) deviation from Debye response under the experimental condition.

dielectric relaxation time constant, $\tau = (\omega^{Z''}_{\text{max}})^{-1}$. Unlike system with high salt content, system with low salt content may be close to Debye relaxation as the distance of $f^{Z''}_{\text{max}}$ and $f^{Z'-Z''}_{\text{cross}}$ are very close, where we noted the frequency $f^{Z''}_{\text{max}} \approx f^{Z'-Z''}_{\text{cross}}$ [*c.f.* Figure 1(c)].

- System with high salt content shows that the distance of $f^{Z''}_{\text{max}}$ and $f^{Z'-Z''}_{\text{cross}}$ are expanding with $f^{Z''}_{\text{max}} < f^{Z'-Z''}_{\text{cross}}$. The system is suffering from the severe accumulation of interacting dipoles at $f^{Z''}_{\text{min}}$ that in the end led to a distribution of relaxation times (deviation of Debye response) [*c.f.* Figure 1(d)].
- **Note:** under Debye relaxation (*i.e.* $f^{Z''}_{\text{max}} = f^{Z'-Z''}_{\text{cross}}$), there are no interactions between dipoles and only one relaxation time, τ with $\omega^{Z''}_{\text{max}} = \omega^{Z'-Z''}_{\text{cross}}$. This is an ideal condition.

We note that the double-logarithmic plot of impedance spectra of PMA-LiClO$_4$ presented in Figure 2(a):

- The system has no maximum resonance in Z'' spectrum at low salt content and one broad maximum resonance is observed in Z'' spectrum of system with high salt content at frequency noted as $f^{Z''}_{\text{max}}$. This indicates no dipolar entities in PMA with low salt content and only appear after adding higher content of salt under the experimental condition [*c.f.* Figure 2(c)].
- Both systems have one intersection point at Z' and Z'' spectrum at a frequency noted as $f^{Z'-Z''}_{\text{cross}}$. The distancing of $f^{Z''}_{\text{max}}$ and $f^{Z'-Z''}_{\text{cross}}$ for binary PMA-salt system cannot be estimated here as $f^{Z''}_{\text{max}}$ for PMA with low salt is out of measurement range, it happens to be at lower frequency range. However, the distance of $f^{Z''}_{\text{max}}$ and $f^{Z'-Z''}_{\text{cross}}$ of PMA with high salt is seen to be wider than PEO at the same composition [*c.f.* Figure 2(b)].
- Unlike PEO, no $f^{Z''}_{\text{min}}$ is noted for both low and high salt systems of PMA. It seems the $f^{Z''}_{\text{min}}$ of both compositions exist at much lower frequency range, most likely at zero frequency, and it cannot be retrieved under this experimental condition.
- The interesting finding in PMA-Li salt system is the existence of distribution of relaxation times after addition of high composition of salt by $f^{Z''}_{\text{max}} < f^{Z'-Z''}_{\text{cross}}$ [*c.f.* Figure 2(d)]. This indicates a large deviation from Debye response and may lead to the conclusion that the orientation of dipolar entities of PMA-LiClO$_4$ are mainly restricted only to local motions.

A step-by-step guideline to estimate characteristic frequencies of impedance using mathematical regression approach aided with commercial graphical software is presented in the Supplementary file 1 (S1). Guideline in S1 is not limited only for impedance but it may be adopted for other electrochemical terms (*e.g.* loss tangent, electric modulus *etc.*) that displays a characteristic frequency as in impedance. This guide is one of the alternative approaches that may be useful for estimation of reproducible results.

Permittivity

The frequency-dependent permittivity spectra of polymer electrolytes *i.e.* PEO-$LiClO_4$ and PMA-$LiClO_4$, studied using EIS are displayed in Figure 3. Permittivity frequently reflects to the ability of a material to store and transfer the charged entities under an applied electric field. ε' reflects to the stored energy (stored dipoles) and ε'' reflects to the dissipated energy (mobile dipoles), for ionic conduction. The relation of permittivity and ionic conductivity of electrolyte can be reflected in Equation (4), where

$$\sigma_{\mathrm{DC}} \propto \omega \cdot \varepsilon'' \tag{4}$$

where the σ_{DC} is directly proportional to ε'' at constant ω, with $\omega = 2\pi f$. Estimation of σ_{DC} was elaborated in Part 1 of this article. Equation (4) tells the ionic conductivity can be estimated easily with permittivity as they are proportionate to each other. Apart from that, Equation (4) also expresses the existence of a power-law dependence in ε'' spectrum at constant σ_{DC} (*i.e.* at low frequency, $\omega_{\min}^{Z''} \ldots \omega_{\max}^{Z''}$), which reads as

$$\varepsilon'' \propto \frac{1}{\omega^{n}} \tag{5}$$

with the exponential of n should be less than or equal to unity ($n \leq 1$). The exponential n represents the slope of a linear regression. It is noted when exponent $n = 1$, it implies to only one relaxation time constant following Debye response. Consequently, when $n < 1$, it indicates a distribution of relaxation times in the system that

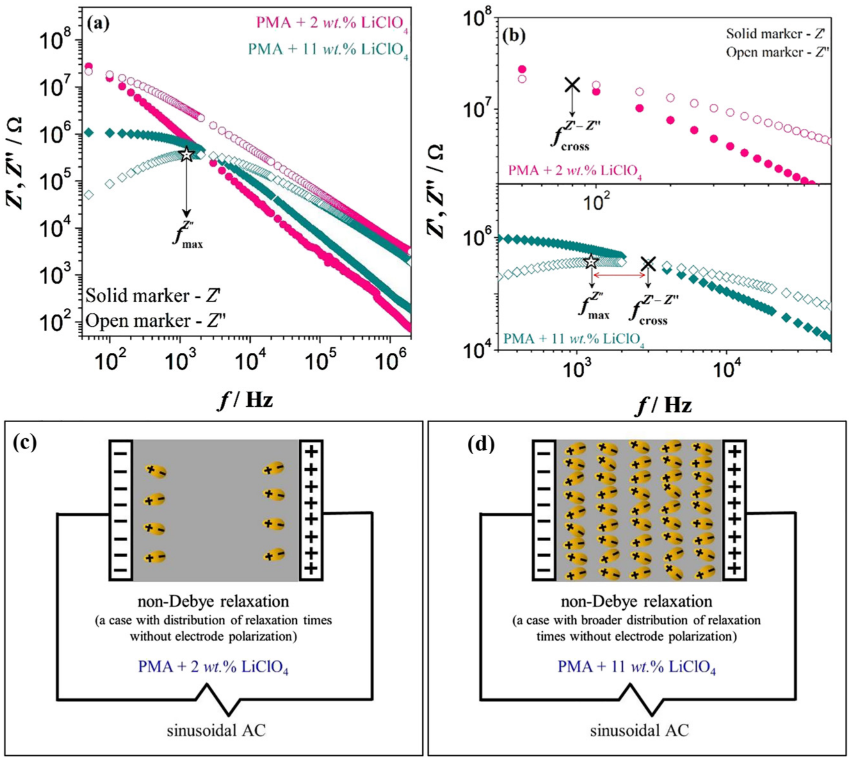

Figure 2: Frequency-dependent impedance spectra of (a) PMA-$LiClO_4$ and (b) zoom-in PMA-$LiClO_4$, and schematic illustration of dipolar entities orientation of the respective systems, where (c) deviation from Debye response and (d) large deviation from Debye response under the experimental condition.

shows deviation from Debye response. The focus of this section is to reveal the significance of power-law dependence in the imaginary part of ε'' in the range of frequency $f_{\min}^{Z''}$ and $f_{\max}^{Z''}$. The interrelations of all basic electrochemical quantities are highly important as they always reflect to their conductance activity.

The double-logarithmic plot of permittivity spectra presented in Figure 3 as:

- all systems have a linear decrease in ε'' in the range of frequency from $f_{\min}^{Z''}$ to $f_{\max}^{Z''}$, which tells the accessibility of power law distribution as displayed in Equation (5).
- the linear regressions in ε'' in the range of frequency $f_{\min}^{Z''}$ and $f_{\max}^{Z''}$ after Equation (5) of Figure 3 yield
  $n = 0.95$ for PEO with 0.5 wt.% of $LiClO_4$
  $n = 0.92$ for PEO with 11 wt.% of $LiClO_4$
  $n = 0.90$ for PMA with 11 wt.% of $LiClO_4$
- The exponential n values of PEO- and PMA-salt reduce with increasing salt content. This points to the increase in the distribution of relaxation times with higher addition of salt. However, we observe a close to Debye relaxation (with $n \approx 1$) for PEO added with low salt content.
- The ε'' increase from ~ 100 (for PEO with 0.5 wt.% of $LiClO_4$) to ~ 3×10^4 (for PEO 11 wt.% of $LiClO_4$) at $f = 50$ Hz with increasing salt content. Similar observation is noted for PMA-$LiClO_4$ system.
- Hence, the ionic conductivities of both polymer electrolytes are seen to be increased with elevating salt content as ε'' permittivity is directly proportional to ionic conductivity at a constant ω, which $\omega = 2\pi f$ [*c.f.* Equation (4)].

Loss tangent

Loss tangent ($\tan\delta$) can be defined as the ratio of mobile and stored charged entities (dipoles) (ratio of $\varepsilon''/\varepsilon'$) of the system. In this spectrum, frequency noted as $f_{\max}^{\delta}$ (due to appearance of maximum resonance in the $\tan\delta$ spectrum at the frequency) can be observed specifically for binary polymer-salt system with existence of frequency noted as $f_{\min}^{Z''}$ in Z'' spectrum. Both characteristic frequencies of respective spectra should be overlapped or close by $(f_{\max}^{\delta} \approx f_{\min}^{Z''})$ if the system follows Debye response.

We note the plot of loss tangent spectra presented in Figure 4 as:

- Figure 4(a) elucidates that $f_{\max}^{\delta}$ of both PEO-$LiClO_4$ systems are less than $f_{\min}^{Z''}$ $(f_{\max}^{\delta} < f_{\min}^{Z''})$ coupled with the increase in distancing of the two frequencies with high salt, leading to distribution of relaxation times. The increasing area under the $\tan\delta$ spectrum also implies to increase in number and strength of dipoles relaxation in the electrolytic system. This is true as the spectrum increases with elevating content of salt. The observation of $f_{\max}^{\delta}$ shifts to higher frequency with elevating salt content for PEO-salt denotes on the electrode polarization is only restricted to local dipoles motion.

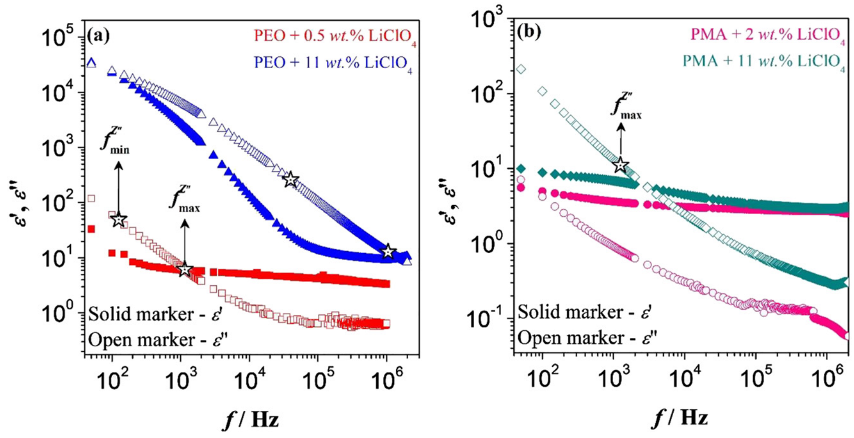

Figure 3: Frequency-dependent permittivity spectra of (a) PEO-$LiClO_4$ and (b) PMA-$LiClO_4$.

- However, these are not seen in PMA-salt. There is no visible maximal resonance in tan δ of PMA-salt as the characteristic frequency may be lying at lower frequency region, apart from the sign of non-existence of electrode polarization at the electrode-electrolyte interface. Only monotonic decrease is observed over the frequency sweep and no dipolar relaxation illuminates. This is consistent with Z'' of PMA-salt where no $f_{\min}^{Z''}$ are seen [*c.f.* Figure 4(b)].

Electric modulus

In general, the interrelation of modulus and impedance can be elucidated as in Equation (1). Hence, dynamically we see electric modulus after Equation (1) as dynamic quantity, where M'' is directly proportional to $\dot{Z}'$ where $\dot{Z}'$ is the time derivative of Z'. Hence, after several manipulations of Equation (1), we see the symmetric formulations that are the central points of the discussion:

$$M'' \propto \omega Z' \tag{6}$$

$$\frac{Z''}{R} \propto \omega \varepsilon' \tag{7}$$

Here, the comparison of modulus and impedance are made in the low-frequency range ($f_{\min}^{Z''} \le f \le f_{\max}^{Z''}$). We denote here the Z'' as the non-Ohmic resistance and M'' is proportional to Ohmic resistance, which is the real part of impedance Z'. Subsequently, Equation (6) demonstrates that imaginary part of modulus points towards electric relaxation or non-local motion of charged entities (flow of charges) in the frequency range of $f_{\min}^{Z''} \le f \le f_{\max}^{Z''}$. This points towards long-range motion of dipoles coupled to segmental motions of chains only occur in the low frequency range. With that, it allows to assume the imaginary part of impedance, shown in Equation (7), denotes the dielectric relaxation only coined to short-range motion of dipoles.

We note here, the plot of electric modulus spectra presented in Figure 5 as:

- PEO-salt exhibits relaxation resonance in the spectra of Z'' and M'' as demonstrated in Figures 1(a) and 5(a), respectively. We observe in PEO, the M'' exhibits a maximum at frequency $f_{\max}^{M''}$. The existence of the maximum (relaxation) denotes the transition of long-range motion in the range of frequencies $f < f_{\max}^{Z''}$ to short-range motion at higher frequency range ($f > f_{\max}^{M''}$), as a consequence from the rapid changes of the external electric field at which the charged entities are unable to response appropriately any more (*c.f.* Figure 5). The frequency $f_{\max}^{M''}$ also moves to lower values for PEO at room temperature. Besides, we see the inequality in the characteristic frequencies where it is always $f_{\max}^{Z''} < f_{\text{cross}}^{Z'-Z''} < f_{\max}^{M''}$, indirectly by chance reflects to dispersion of relaxation times, deviation from Debye response, especially for PEO with high salt.

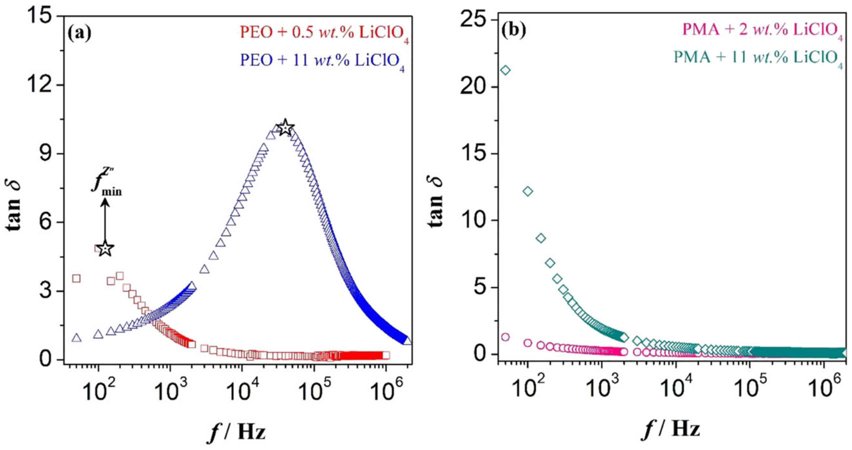

Figure 4: Frequency-dependent loss tangent spectra of (a) PEO-LiClO$_4$ and (b) PMA-LiClO$_4$.

- These characteristic frequencies also provide more information on the transport properties of the charged entities in the system. We note here the charge transport for PEO is mainly governed by short-range irregular (localized) motion as the dielectric relaxation is more dominant [*c.f.* Figure 5(a)]. In other words, the conductance activity PEO-salt is dominated by short-range or local motions of dipoles and long-range motions only have minor influence on the system.
- Unlike PEO-salt, PMA-salt system only shows the conducting behavior after addition of sufficiently high salt content. The system possesses a large deviation from Debye response, as the large difference in the characteristic frequencies $f^{Z''}_{\text{max}} < f^{Z'-Z''}_{\text{cross}} < f^{M''}_{\text{max}}$ is always noted that indicates to dispersion of relaxation times. Moreover, the frequency $f^{M''}_{\text{max}}$ does not moves to lower value like PEO even added with same composition of salt at room temperature. Hence, the system is seen to be bounded to short-range irregular motions of dipoles only.

Conductivity

We observe the complex conductivity σ^* is highly related to dynamic complex permittivity in the linear range of $f^{Z''}_{\text{min}}$ and $f^{Z''}_{\text{max}}$, where it is given by

$$\sigma^* = \epsilon_o \epsilon^* \tag{8}$$

Equation (8) shows the direct relationship of real and imaginary parts of conductivity to imaginary and real parts of permittivity, respectively

$$\sigma' \propto \omega \varepsilon'' \quad \sigma'' \propto \omega \varepsilon' \tag{9}$$

ε'' is related to dissipation of energy for conduction. Hence, the σ' can be seen as constant ($\sigma' \approx const$) or linear in the frequency limit of $f^{Z''}_{\text{min}}$ and $f^{Z''}_{\text{max}}$ as illustrated in Figure 6. Extrapolation in the range of $f^{Z''}_{\text{min}}$ and $f^{Z''}_{\text{max}}$ yields $\sigma' \approx const$ and this is noted as the DC conductivity (σ_{DC}) (*c.f.* Figure 6). For frequencies $f < f^{Z''}_{\text{min}}$, we may see some system possess increase in σ'' and decrease in σ'. This implies to occurence of electrode polarization leading to conductivity decreases, respectively.

σ' represents dissipation of energy due to flow of charges/dipoles, and this is closely interlinked to conduction, whereas σ'' reflects to the amount of stored energy in the system coming from the electric field. In most cases, the long-range transport of charged entities only contributes minor influence on the conductivity. We would say the conductivity is preferably ruled by dielectric response of the system in range of $f^{Z''}_{\text{max}} < f^{Z'-Z''}_{\text{cross}}$. Figure 6 denotes the slight increase in conductivity σ' in the range of $f^{Z''}_{\text{min}}$ and $f^{Z''}_{\text{max}}$, indicating deviation from Debye relaxation, especially at PEO and PMA with high salt content. The low frequency resonance $f^{Z''}_{\text{min}}$ of PMA

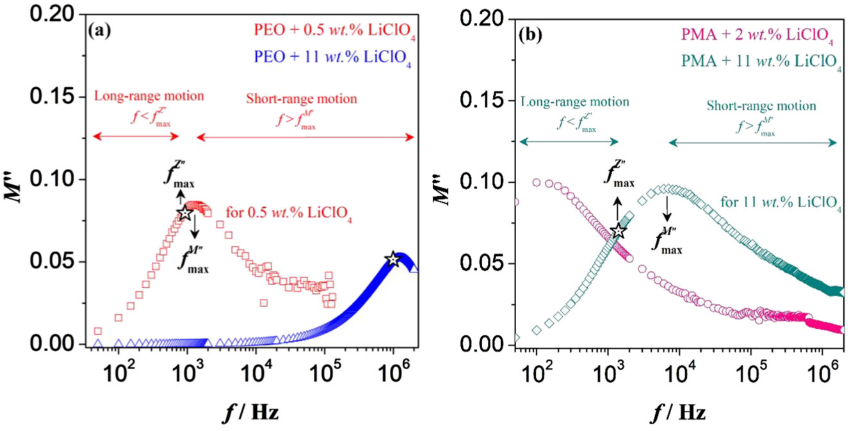

Figure 5: Imaginary modulus *versus* frequency spectra of (a) PEO-$LiClO_4$ and (b) PMA-$LiClO_4$.

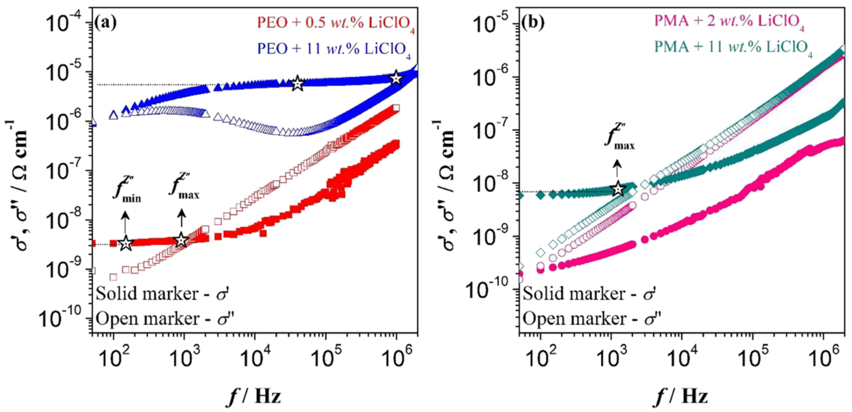

Figure 6: Frequency-dependent conductivity spectra of (a) PEO-LiClO$_4$ and (b) PMA-LiClO$_4$. The dotted line marks as DC conductivity (σ_{DC}) in the range of $f_{min}^{Z''}$ and $f_{max}^{Z''}$.

is not accessible under this experimental procedure because it lies at very low frequency region. Thus, we may see the $\sigma' \approx const$ and σ'' aprroaching zero ($\sigma'' \to 0$) in the range of f approaching zero ($f \to 0$) for PMA system as there is no storage of charges in the interfacial region [*c.f.* Figure 6(b)].

Conductivity of PMA-salt system exhibits very low conductivity σ' in the low frequency range as compared to PEO-salt system (at the same content). Conductivity of PMA at high salt content mostly acts comparatively same as PEO at low salt content. PMA only acts as insulator with tiny fraction of salt. It becomes slight electrically active only after addition of high content of salt unlike PEO [*c.f.* Figure 6(a)]. As conclusion, the conductivities of binary polymer-salt system under discussion are seen to be dependent of polymer as well as salt content as seen from the overall phenomenon response of electrochemical aspects.

Conclusion

Two different classes of systems, *i.e.* high molar mass semi-crystalline PEO and low molar mass amorphous PMA with addition of LiClO$_4$, were employed for discussion on the phenomenological response of imaginary part of impedance spectrum (Z''), imaginary part of permittivity (ε''), tan δ (imaginary/real of permittivity), the imaginary part of electric modulus (M''), and the real part of conductivity (σ'). We observe there are interactions between the salt molecules and PEO chains leading to dipolar entities, but they relaxed in random manner. Therefore, under the effect of external electric field, we see PEO-salt system as a polymer electrolyte because even with a tiny fraction of salt molecules dissolved in, the system becomes electrically conductive. PMA-salt system only become slightly conductive after addition of high salt content; however, it still cannot display electrode polarization or electric relaxation because the dipoles are immobilized (restricted to local motion only). Hence, in the classic sense, PMA-salt does not form a good polymer electrolyte. The primary intention of this article is to highlight on how to discuss this difficult matter in simpler manner in order to assist beginners and young researchers to be familiar on the other aspects of electrochemical impedance spectroscopy, beside serving as an alternative reference for course instructors to coach their students on the subject matter.

Supplementary Information

Two supplementary files (i.e **S1** – A step-by-step guideline to estimate characteristic frequencies in impedance using mathematical regression with commercial graphical software, **S2** – PowerPoint slide: Basics of Teaching Electrochemical Impedance Spectroscopy of Electrolytes for Ion-rechargeable Batteries) are provided separately for educational, practical, and self-learning purposes.

Acknowledgments: The authors would like to express appreciation to Mdm. Amirah Hashifudin for providing impedance result of PEO with 0.5 wt.% of $LiClO_4$.

Author contributions: All the authors have accepted responsibility for the entire content of this submitted manuscript and approved submission.

Research funding: The authors would like to express the greatest appreciation to Universiti Teknologi MARA (UiTM), Malaysia for granting LESTARI Grant [600-IRMI/MyRA/5/3/ LESTARI (1072/2017)] and Ministry of Education, Malaysia for providing MyBrain15 (MyPhD) to financially support some experimental work of this article.

Conflict of interest statement: The authors declare no conflicts of interest regarding this article.

References

Abdul Halim, S. I., Chan, C. H., & Apotheker, J. (2020). Basics of teaching electrochemical impedance spectroscopy of electrolytes for ion-rechargeable batteries – part 1: a good practice on estimation of bulk resistance of solid polymer electrolytes. *Chemistry Teacher International*. https://doi.org/10.1515/cti-2020-0011.

Abdul Halim, S. I., Chan, C. H., & Kammer, H.-W. (2019). About glass transition in polymer-salt mixtures. *Polymer Testing*, *79*, 105994.

Abraham, K. M., & Jiang, Z. (1996). A polymer electrolyte-based rechargeable lithium/oxygen battery. *Journal of the Electrochemical Society*, *143*(1), 1–5.

Agrawal, R. C., & Pandey, G. P. (2008). Solid polymer electrolytes: Materials designing and all-solid-state battery applications: An overview. *Journal of Physics D: Applied Physics*, *41*(22), 223001.

Alloin, F., D'Aprea, A., El Kissi, N., Dufresne, A., & Bossard, F. (2010). Nanocomposite polymer electrolyte based on whisker or microfibrils polyoxyethylene nanocomposites. *Electrochimica Acta*, *55*(18), 5186–5194.

Armand, B. (1986). Polymer electrolytes. *Annual Review of Materials Science*, *16*, 245–261.

Berthier, C., Gorecki, W., Minier, M., Armand, M. B., Chabagno, J. M., & Rigaud, P. (1983). Microscopic investigation of ionic conductivity in alkali metal salts-poly(ethylene oxide) adducts. *Solid State Ionics*, *11*(1), 91–95.

Billah, S. M. R. (2019). Dielectric polymers. *Functional polymers, polymers and polymeric Composites: A reference series* (pp. 241–288). https://doi.org/10.1007/978-3-319-95987-0_8.

Bode, H. W. (1945). Network analysis and feedback amplifier design. *Bell Telephone Laboratories series*.

Chan, C. H., & Kammer, H.-W. (2008). Properties of solid solutions of poly(ethylene oxide)/epoxidized natural rubber blends and $LiClO_4$. *Journal of Applied Polymer Science*, *110*, 424–432.

Chan, C. H., & Kammer, H. W. (2015). Polymer electrolytes—relaxation and transport properties. *Ionics*, *21*(4), 927–934.

Chan, C. H., & Kammer, H. W. (2016). On dielectrics of polymer electrolytes studied by impedance spectroscopy. *Ionics*, *22*(9), 1–9.

Chan, C. H., & Kammer, H. W. (2018). Characterization of polymer electrolytes by dielectric response using electrochemical impedance spectroscopy. *Pure and Applied Chemistry*, *90*(6), 939–953.

Chan, C. H., & Kammer, H. W. (2020). Low frequency dielectric relaxation and conductance of solid polymer electrolytes with PEO and blends of PEO and PMMA. *Polymers*, *12*, 1–19.

Chan, C. H., Kammer, H. W., Sim, L. H., Yusoff, S. N. H. M., Hashifudin, A., & Winie, T. (2014). Conductivity and dielectric relaxation of Li salt in poly(ethylene oxide) and epoxidized natural rubber polymer electrolytes. *Ionics*, *20*(2), 189–199.

Chan, C. H., Sulaiman, S. F., Kammer, H. W., Sim, L. H., & Harun, M. K. (2011). Thermal properties of epoxidized natural rubber-based polymer blends. *Journal of Applied Polymer Science*, *120*(3), 1774–1781.

Chen, X. C., Sacci, R. L., Osti, N. C., Tyagi, M., Wang, Y., Keum, J. K. & Dudney, N. J. (2019). Study of the segmental dynamics and ion transport in polymer-ceramic composite electrolytes by quasi-elastic neutron scattering. *Molecular Systems Design and Engineering*, 1–7.

Chen, X. C., Sacci, R. L., Osti, N. C., Tyagi, M., Wang, Y., Keum, J. K. & Dudney, N. J. (2021). Study of the segmental dynamics and ion transport of solid polymer electrolytes in the semi-crystalline state. *Frontiers in Chemistry*, *8*, 592604(1)–592604(8).

Christie, A. M., Lilley, S. J., Staunton, E., Andreev, Y. G., & Bruce, P. G. (2005). Increasing the conductivity of crystalline polymer electrolytes. *Nature*, *433*(7021), 50–53.

Das, A., Thakur, A. K., & Kumar, K. (2013). Exploring low temperature Li^+ ion conducting plastic battery electrolyte. *Ionics*, *19*(12), 1811–1823.

Halim, S. I. A., Chan, C. H., & Winie, T. (2017). Thermal, conductivity and molecular interaction studies of poly(ethylene oxide)/poly(methyl acrylate) solid polymer electrolytes. *Macromolecular Symposia*, *371*(1), 114–124.

Harun, F., Chan, C. H., & Winie, T. (2017). Influence of molar mass on the thermal properties, conductivity and intermolecular interaction of poly(ethylene oxide) solid polymer electrolytes. *Polymer International*, *66*(6), 830–838.

Hassoun, J., & Scrosati, B. (2010). A high-performance polymer Tin Sulfur Lithium ion battery. *Angewandte Chemie International Edition*, *49*(13), 2371–2374.

Kammer, H. (2017). Dielectric relaxation in PEO-based polymer electrolytes. *Ionics*, *24*, 1415–1428.

Karim, S. R. A., Sim, L. H., Chan, C. H., & Ramli, H. (2015). On thermal and spectroscopic studies of poly(ethylene oxide)/poly(methyl methacrylate) blends with lithium perchlorate. *Macromolecular Symposia*, *354*(1), 374–383.

Li, Q., Chen, J., Fan, L., Kong, X., & Lu, Y. (2016). Progress in electrolytes for rechargeable Li-based batteries and beyond. *Green Energy & Environment*, *1*(1), 18–42.

Martwiset, S., Yavuzcetin, O., Thorn, M., Versek, C., Tuominen, M., & Coughlin, E. B. (2009). Proton conducting polymers containing 1H-1,2,3-triazole moieties. *Journal of Polymer Science, Part A: Polymer Chemistry*, *47*(1), 188–196.

Mead, D. J., & Fuoss, R. M. (1942). Electrical properties of solids. XIII. polymethyl acrylate, polymethyl methacrylate, polymethyl-α-chloracrylate and polychloroethyl methacrylate. *Journal of the American Chemical Society*, *64*(10), 2389–2393.

Pratap, R., & Chandra, S. (2013). Ion transport studies in PEO:NH_4ClO_4 polymer electrolyte and its composite with Al_2O_3. *Polymer Bulletin*, *70*(11), 3075–3089.

Pulst, M., Balko, J., Golitsyn, Y., Reichert, D., Busse, K., & Kressler, J. (2016). Proton conductivity and phase transitions in 1,2,3-triazole. *Physical Chemistry Chemical Physics*, *18*(8), 6153–6163.

Scrosati, B., Croce, F., & Panero, S. (2001). Progress in lithium polymer battery R&D. *Journal of Power Sources*, *100*(1–2), 93–100.

Wang, Y., Fan, F., Agapov, A. L., Saito, T., Yang, J., Yu, X., …, Sokolov, A. P. (2014). Examination of the funadamental relation between ionic transport and segmental relaxation in polymer electrolytes. *Polymer*, *55*, 4067-4076.

Wang, B. H., Xia, T., Chen, Q., & Yoa, Y. F. (2020). Probing the dynamics of Li^+ ions on the crystal surface: A solid-state NMR study. *Polymers*, *12*, 391(1)–391(12).

Supplementary Material: The online version of this article offers supplementary material (https://doi.org/10.1515/cti-2020-0018).